Numerical Analysis of Fluid Flow and Heat Transfer for Different Fin Designs and Arrangements of Ceramic Plate-Fin High Temperature Heat Exchanger – Part I

Vijaisri Nagarajan[a], Yitung Chena*, Qiuwang Wangb[b], Ting Ma[b]

a Department of Mechanical Engineering, University of Nevada, Las Vegas, NV 89154-4027, USA

[b] Key Laboratory of Thermo-Fluid Science and Engineering, MOE, Xi'an Jiaotong University, Xi'an, Shaanxi, 710049, China

Abstract - In this study numerical analysis is carried out for four different types of fins namely rectangular, triangular, inverted bolt fins and ripsaw fins for staggered fin arrangement. The obtained results are compared with each other, and the design with best heat transfer and minimum pressure drop is selected. The working fluids used in the model are sulfur trioxide, sulfur dioxide, oxygen and water vapor. The operating pressure is 1.5 MPa and the operating temperature ranges from 973 K to 1223 K.

From the results it was found that the ripsaw fin design with thickness of 0.00005 m gives a good heat transfer rate with minimum pressure drop. The inverted bolt fins has the highest pressure drop due to the flow disturbances caused by the arrangement of the fins. The pressure drop and the heat transfer obtained for the rectangular and triangular fins are similar to each other. Friction factor, Colburn j- factor and dimensionless numbers like Nusselt number, Schmidt number are calculated for all the models. The average Nusselt number obtained for the ripsaw fin design with thickness of 0.00005 m for the top and bottom arrangement is 3.197. The friction factor for the ripsaw fins for the top and bottom arrangement is 0.522.

Keywords - Heat transfer enhancement factor, Ceramic Plate-Fin (PFHE) Heat Exchanger, Nusselt number, Schmidt number, pressure drop.

I. INTRODUCTION

Compact heat exchangers (CHE) plays an important role in the field of aerospace, transportation, nuclear and other industries. The need for lightweight, space saving and economical heat exchangers have driven to the development of compact heat exchangers. Surface area density of greater than $700 m^2/m^3$ is achieved by incorporating fins, ribs tec. The book by Hesselgreaves [1] describes different types of compact heat exchangers like plate-fin heat exchangers, spiral heat exchangers, printed circuit heat exchangers, tube fin heat exchangers etc. A plate-fin heat exchanger is a form of compact heat exchanger made of block of alternating layers of corrugated fins separated by parting sheets. Surface interruption prevents the continuous growth of the thermal boundary layer by periodically interrupting it. Thus the thicker thermal boundary layer which offers high thermal resistance to heat transfer are maintained thin and their resistance to heat transfer is reduced. In a plate-fin heat exchanger, fins are easily rearranged resulting in cross-flow, counter-flow, cross-counter-flow or parallel flow arrangements. From the research done by Kayansayan [2] the effect of the performance of plate-fin and tube cross-flow heat exchangers due to the outer surface geometry was considered.

In this study 10 geometrical configurations were tested and the Reynolds number was varied from 2,000 to 30,000. The results showed that the heat transfer coefficient strongly depends on the finning factor ε and the value of ε increases with decrease in j-factor. Ranganayakaulu & Seetharamu [3] carried out an analysis of a cross-flow compact plate-fin heat exchanger for the combined effects of two-dimensional longitudinal heat conduction through the exchanger wall, flow non-uniformity and temperature distribution was carried out using the finite element method. The exchanger effectiveness and thermal deterioration due to these effects were studied for various design and operating conditions. Wen & Li [4] proposed a study in order to enhance the uniformity of flow distribution. In their study an improved header configuration of plate-fin heat exchanger was proposed. The results showed that the fluid flow misdistribution was very severe in the direction of header length for the conventional header used in the industry due to poor header configuration.

Manglik & Bergles [5] studied the heat transfer and pressure drop correlations for the rectangular offset strip-fin compact heat exchanger. The f and j parameters were also found for laminar, transition and turbulent flow regimes. Steady state three-dimensional numerical model was used to study the heat transfer and pressure drop characteristics of an offset strip-fin heat exchanger by Bhowmik & Lee [6] Three different performance criteria for heat exchangers were tested for different fluids and the appropriate performance criteria for Pr = 7 and Pr = 50 were found to be JF (thermal-hydraulic performance factor) and j/f1/3.

Research has been carried out by Ma et al. [7] to find heat transfer and pressure drop performances of ribbed channels in the high temperature heat exchanger. From the results it was found that the Nusselt number and the friction factor were unsuitable to compare heat transfer and pressure drop performances at different temperature conditions. Schulte-Fischedick et al. [8] proposed a ceramic high temperature plate-fin heat exchanger for externally fired combustion process. Thermal performance and pressure drop in ceramic heat exchanger was evaluated using CFD simulations by Monteiro et al. [9]. Correlations for the Colburn and the friction factors for the Reynolds number ranging from 500 to 1500 were evaluated. Simulations with conjugate heat transfer were conducted and the results show the influence of mass flow rate on pressure drop and effectiveness of the heat exchanger. Ponyavin et al. [10] carried out a numerical analysis on the three-dimensional computational model of the ceramic high-temperature heat exchanger to investigate fluid flow, heat transfer, and chemical reaction and stress analysis within the decomposer. A decomposition rate of 0.515% was achieved for SO_3 using this design.

In this study numerical analysis of ceramic plate fin high temperature heat exchanger was carried out to investigate the fluid flow and heat transfer for different fin designs and fin arrangements. This study is an extension of the work done by Nagarajan et al. [11]. In order to save computational space and time a single channel model of the heat exchanger is modeled and studied. The main operating parameters for the heat exchanger design models for the current study are taken from the research done by Ponyavin et al. [10].

II.   GEOMETRY OF THE MODEL AND MATERIAL PROPERTIES

In this study three-dimensional study of the fluid flow and heat transfer on four type of fins namely rectangular, triangular, inverted bolt fins and ripsaw fins for top and bottom arrangement is carried out. The computer aided geometry (CAD) geometry for all the models are modeled in Solid works [12] and simulations are carried out in ANSYS FLUENT 14.5.

 The geometry and dimensions for the current study is taken from the work done by Ponyavin et al. [10] and from his study it was found that mass flow rate in all channels can be made almost uniform with a proper design of manifold channels. Hence by applying that concept a single channel model is developed to reduce computational time and memory. Single-banking configuration is used where in the hot and the cold plates are stacked alternatively.

The current study has hot fluid channel, cold fluid channel and two silicon carbide (SiC) solid regions. Helium fluid flows through the hot channel placed above the solid region and mixture of sulfur trioxide, sulfur dioxide, oxygen and water vapor flows through the cold fluid channel which is placed between the two solid regions. The flow is counter flow where the hot and the cold fluids enter the model from –x and +x directions and exit in the +x and –x directions, respectively. Figure 1 shows the geometry and dimensions of the single channel of plate fin heat exchanger.
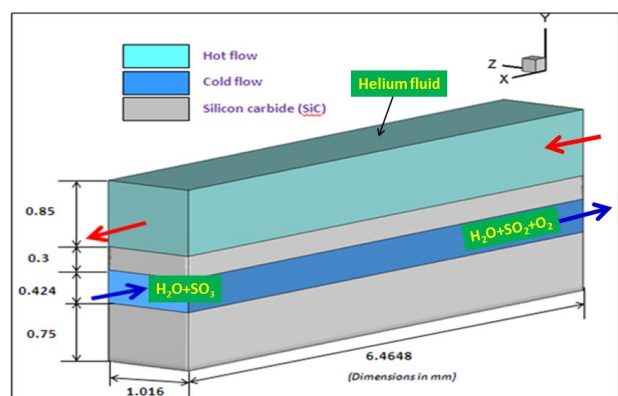

Fig .1. Geometry and dimensions of the channel

To enhance the thermal performance of the PFHE many fin designs are explored and studied. Table 1 shows the dimensions of all the fins

Table 1. Dimensions of various fins

Geometry	Definition
Rectangular fins	Height = 0.4 mm, length = 0.4 mm, width = 0.2 mm
Triangular fins	Height = 0.3 mm, breadth = 0.2 mm, length = 0.4 mm
Inverted bolt type fins	Diameter of top cylinder = 0.2 mm, diameter of bottom cylinder = 0.4 mm
Ripsaw fins	Larger height of the rectangle = 0.3 mm, smaller height of the rectangle = 0.15 mm, thickness = 0.05 m

In order to avoid backflow and provide entrance zone for each channel no fins are placed near the inlet and the outlet region on the cold channel. A study was carried out by increasing the length of the inlet and outlet to 5, 10 and 15 times the hydraulic diameter. At 10 times the hydraulic diameter the flow becomes fully developed and hence the length of the inlet and outlet are taken to be 10 times the hydraulic diameter. The material properties, boundary and operating conditions are taken from the work done by Nagarajan et al.

III. NUMERICAL METHOD AND ALGORITHM

The finite volume method is one of the most versatile discretization techniques used in CFD. The governing equations are solved in the Cartesian coordinate system using a control volume finite difference method that is similar to the approach introduced by Patankar [14]. ANSYS FLUENT [13] a commercial CFD program based on the finite volume method is among the most powerful packages of existing software used for solving fluid flow and heat transfer problems. The pressure-based segregated solution algorithm is used for the given problem. It can be simply described as the process of solving the governing equations in a sequential order as opposed to simultaneously as with a coupled solver.

The geometry of the model is meshed in ANSYS WORKBENCH [13] mesh generator. Hexahedral elements are used for meshing. The mesh is refined near the walls particularly for the cold flow channel with fins. The mesh refinement near the wall helps in calculating the fluid flow and heat transfer properties accurately. In order to check the mesh dependence on fluid flow and heat transfer properties, the grid independent study was done for both staggered and top and bottom arrangement. From the study,

optimum nodes with difference in pressure drop and heat transfer of less than 5% is selected for further study. Around 481,558 cells, 1,496,152 faces and 532,599 nodes are selected for further study for all the cases. The friction factor, the Colburn factor and the Prandtl number are calculated using the formula shown below:

$$f = \frac{\left(\frac{\Delta P}{L}\right) * D_h}{(0.5 \cdot \rho \cdot U^2)} \tag{1}$$

$$j = \frac{\overline{Nu}}{Re \cdot Pr^{\frac{1}{3}}} \tag{2}$$

$$Pr = \frac{\mu \cdot C_p}{K} \tag{3}$$

The Schmidt number which is the ratio of the viscous diffusion rate to the mass diffusion rate is calculated based on the average temperature of the reacting channel. The validation of the fluid flow and heat transfer for the rectangular and ripsaw fins was carried out in the previous study done by Nagarajan et al. [11]. The friction factor was compared with the published result by Manson [15] and the Colburn factor was compared with the correlation published by Wieting [16]. The obtained CFD result was in good agreement with the published result and the slight offset is due to the difference in the dimensions of the geometry. Since the numerical results agree closely with the published results and follow the same trend, further research is carried out for the selected design.

IV. RESULTS AND DISCUSSIONS

In this paper studies are done to enhance the heat transfer rate by arranging the fins in the staggered manner. The single channel model with rectangular fins, triangular fins, inverted bolt fins and ripsaw fin with thickness of 0.00005 m are studied in this research. The fluid flow and heat transfer results were discussed in detail in the following.

A. Staggered Arrangement

1. Case 1 (Single Channel Model with Rectangular Fins)

The heat transfer surface area for the staggered rectangular fins is 2.25602·10-5 m^2 and triangular fins is 2.2058·10-5 m^2. The obtained heat transfer rate is high for the staggered arrangement. The obtained

pressure drop for the staggered rectangular and triangular fins is 28.41 Pa and 23.07 Pa, respectively. Due to the staggered arrangement of the fins there is more recirculation and hence higher pressure drop and friction factor are obtained. There is a significant increase in the friction factor for both the fins. The friction factor for rectangular fin is 0.894 and the friction factor for the triangular fin is 0.725. The average Nusselt number and the Colburn j-factor for the rectangular and triangular fins are 3.205, 0.016, and 3.235, 0.016, respectively. The Schmidt number for staggered rectangular and triangular fins is 0.316 and 0.316, respectively.

Flow over staggered rectangular plates produces recirculation in the wake region. In the wake which is formed downstream of the fin the heat transfer is decreased due to the flow disturbances caused by the fins. Relatively low heat transfer distributions are found immediately behind the fin because of flow recirculation with low local velocity. The strong recirculation zone is found behind the fins where the shear layer separates and rolls into vortices. There is no secondary vortex and only one recirculation zone is formed in the wake region. The length of the recirculation region increases with the increase in the Reynolds number. The recirculation region is located at 0.00154 m and the reattachment region of the shear layers is located at 0.00210 m. The velocity streamline for the staggered rectangular fins is shown in Figure 2.
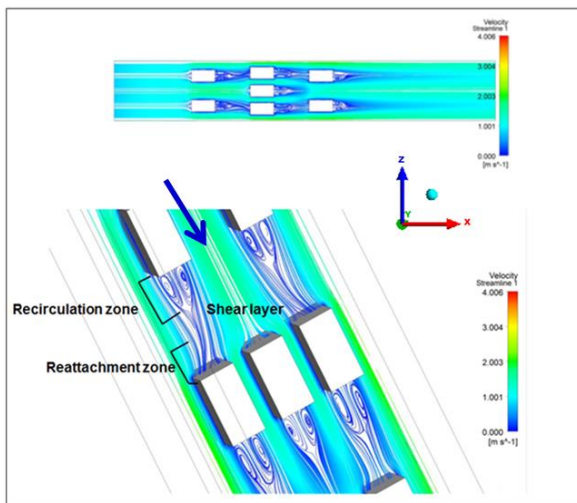

Fig .2. Velocity streamline for single channel model with staggered rectangular fins along y-plane at y=0.003 m and bottom solid regions

The velocity streamline along the z-plane from Figure 3 shows the recirculation zone behind the fins. It can

be seen that recirculation zone for the first and the third plane are formed at the rear end of the second row of fins or the before the start of the third row of fins. This is due to the staggered arrangement of the fins. The z-plane is created at a distance of three-fourth of the first and the third fin and near the edge of the second fin. The recirculation vortex is formed in the wake region immediately behind the first and the third fin. Since the fin thickness is very small behind the second fin no vortices are formed behind the second fins. The shear layers continue from the second fin and they separate and form recirculation zone before the start of the third fin for the first and the third z-plane. Another vortex is formed in the wake region of the third fin and thereafter the shear layers reattach and the flow becomes stable without much fluctuation.
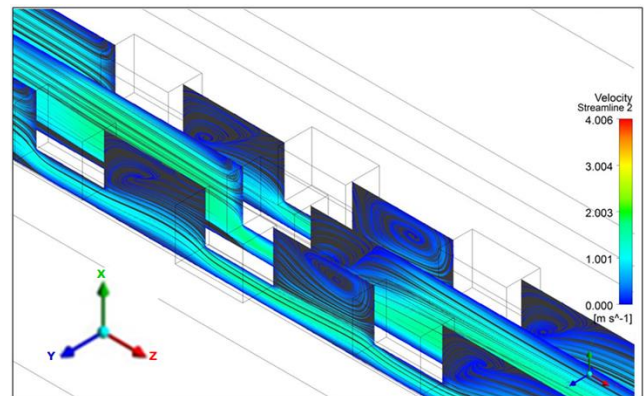

Fig .3. Velocity streamline for single channel model with staggered rectangular fins along z-plane at z=0.0015 m

Figure 4 shows the velocity and local heat transfer coefficient for the single channel model with staggered rectangular fins. The velocity of the fluid decreases from 0.800 m/s and it reaches minimum at the stagnation point P1. The velocity at the stagnation point is 0.101 m/s. The velocity reaches maximum at P2 where the fluid flows without any disturbance and is about 0.975 m/s. The velocity decreases as the fluid travels to the wake region of the fins. The velocity starts decreasing from P3 and becomes minimum at P4. Again the velocity increases and it becomes maximum at P7. The process repeats till the end of the third fin and then the velocity becomes stable till the fluid reaches the outlet. The heat transfer characteristics influenced by the generation of vortex and wake are observed similar to the uniform arrangement of the fins. The heat transfer coefficient is high at point near to the hot solid wall. The heat transfer rate is greatly enhanced due to the fin arrangement and the flow disturbance caused by

the fins. The heat flux is high near the wall and decrease near the bottom region of the fins. The heat transfer coefficient is low at fluid points near the fin bottom. The reason is due to the points are placed away from the hot solid wall and the heat is dissipated by the moving fluid.

The temperature difference is high at points away from the wall and the heat flux is less at these points. After the end of the third fin the heat transfer coefficient increases without much fluctuation till it reaches the outlet. There is increase in heat transfer as the fluid reaches the outlet due to the counterflow arrangement of the heat exchangers.
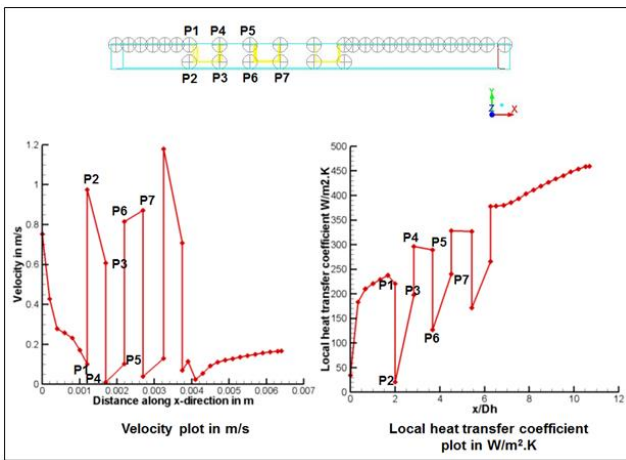
Fig .4. Velocity and local heat transfer coefficient for single channel model with staggered rectangular fins

2. Case 2 (Single Channel Model with Inverted Bolt Fins)

The inverted bolt fins gives a good heat transfer rate compared to all the other cases studied here. The obtained pressure drop for inverted bolt fin case is 31.64 Pa and the friction factor obtained is 0.996. Due to the recirculation and the vortex formed in the fins the obtained pressure drop and the friction factor for the fins are relatively high. The obtained maximum velocity in the fins is 2.027 m/s and the average inlet velocity is 0.8 m/s. The obtained average Nusselt number for the staggered inverted bolt fins is 3.418 and the Colburn j-factor is 0.017. The obtained Schmidt number for the staggered inverted bolt fins is 0.315. The pressure that drives the fluid is the static pressure and the resistance offered to the fluid by the tube causes the pressure drop as the fluid moves towards the exit.

The streamline velocity for the staggered inverted bolt fin is shown in Figure 5. Horseshoe vortices are

formed around the cylinder and the pressure increases at the stagnation point. As the fluid flows around the cylinder shear layer separates and forms vortices behind the fins. Recirculation zone occurs at the wake region behind the cylinder. The vortices formed on the first and the third rows are symmetrical and there are two vortices one rotating in clockwise and the other in counter clockwise direction. Since there are three large cylinders in the second row, the vortices formed are not symmetrical. From Figure 5 the vortices can be found in the wake region on the first and third row of the fins but no recirculation is found in the second row of the fins.

Along the middle z-plane strong recirculation zone is found in the wake region. Since there are more recirculation zones found in the staggered arrangement the obtained pressure drop and friction is high compared to the uniform arrangement. The recirculation region of the staggered inverted bolt fins is located at 0.000957 m and the reattachment region of the shear layer is located at 0.00197 m.
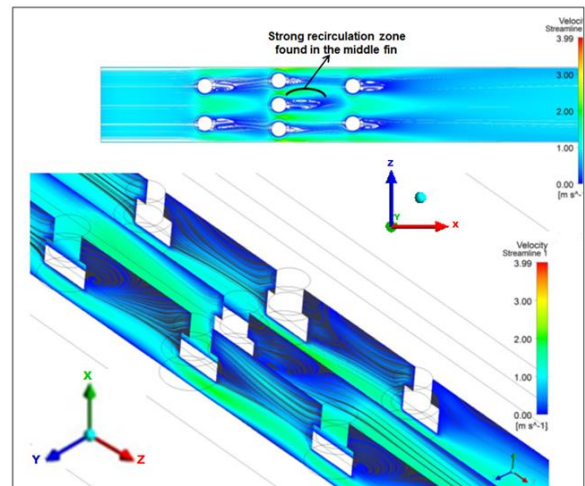

Fig .5. Velocity streamlines for the single channel model with staggered rectangular fins at y=0.003 m and z=0.0048 m

Figure 6 shows the velocity and heat transfer coefficient plot for the staggered inverted bolt fins. The velocity of the fluid decreases and it reaches minimum at P1. P1 is the stagnation point where the pressure is high and the velocity is low. The velocity increases from P2 and it becomes high at P3. The pressure is low at P2 and it starts increasing as the fluid travels to the rear of the cylinder. The velocity is minimum at P4 and the pressure is high at the point due to the adverse pressure gradient. Also the increase in pressure is due to the formation of the

recirculation zone in the wake of the fins. Again as the fluid moves towards the second fin the velocity increases and the pressure decreases until it reaches the wake region of the fins. The velocity is maximum at the end of the second fin due to the staggered arrangement of the fins and there is more space for the fluid to flow without any disturbance. The local heat transfer coefficient is high at points (P1, P4, etc.) near the top solid wall.

The heat flux is high at the top solid wall and it decreases at places away from the top solid wall or near the bottom region of the fins. After P4 the local heat transfer coefficient decreases due to the recirculation formed in the wake region of the fins. The local fluid velocity is low at these points which decrease the heat transfer rate. The temperature and local heat transfer coefficient are low at points (P2, P3 etc.) away from the hot solid wall. After the third fin the local heat transfer coefficient increases without much fluctuation till it reaches the outlet.
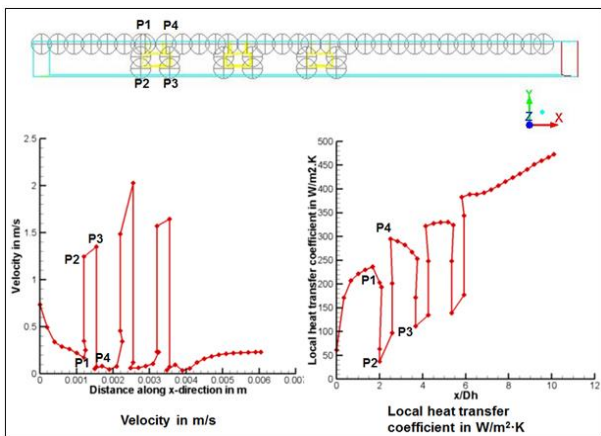

Fig .6. Velocity and local heat transfer coefficient for single channel model with staggered inverted bolt fins

3.   Case 3 (Single Channel Model with Staggered Ripsaw Fin of Thickness 0.00005 m)

The single channel model with staggered ripsaw fins of thickness 0.00005 m gives a good heat transfer rate with reasonable pressure drop. The obtained pressure drop and friction factor are 16.59 Pa and 0.522, respectively. The pressure drop increases by about 1.4 Pa between the uniform and the staggered arrangement of the fins. The obtained heat transfer rate for the staggered ripsaw fin is 0.483 W and the average Nusselt number is 3.404. The obtained Colburn j-factor is 0.017. The average heat transfer coefficient increases from 211.18 W/m²·K to 223.61 W/m²·K. The Schmidt number obtained is 0.315. The

obtained velocity streamlines show that there is no recirculation formed in the wake region. Since the fins are extremely thin and placed close to each other there are no vortices formed in this type of fin arrangement. The heat transfer rate is increased by the increase in the heat transfer surface area. Figure 7 shows the velocity streamline along the y and z-planes.
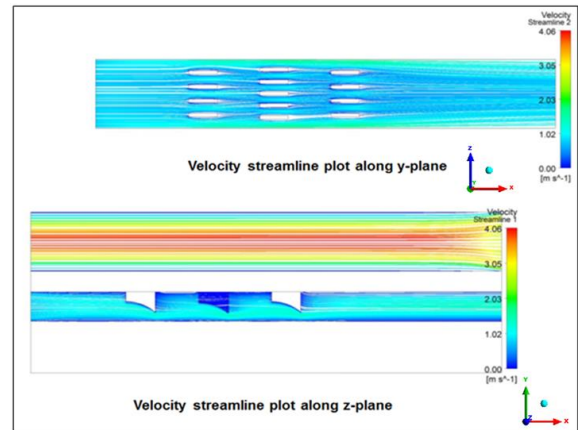

Fig .7. Velocity streamline for single channel model with staggered ripsaw fin with thickness of 0.00005 m at y=0.0037 m and z=0.0047 m

Figure 8 shows the pressure and local heat transfer coefficient for the staggered ripsaw fins with thickness of 0.00005 m. The pressure changes decreases from the inlet until it reaches the fins at P1. At this point the velocity is low due to the stagnation region and after this point the fluid flow around the fins and the flow separation starts. The pressure is low at P2 since there is no obstacle and the velocity is high at this point. As the fluid reaches the rear of the fins there will be a wake region where the pressure increases.

Eventhough there is no recirculation zone in this fin arrangement the pressure increases behind the fins and the velocity decreases due to the obstacles and the narrow space between the fins. This process continues until the fluid reaches the third fin and the flow increases till it reaches the outlet. Due to the resistance offered to the flow the pressure decreases as the fluid moves from the inlet to the outlet. The local heat transfer coefficient is high at points near the hot solid wall and is low at P2 away from the wall. In between P3 and P4 the local heat transfer coefficient decreases due to the decrease in local fluid velocity. The local heat transfer coefficient does not change a lot after the third fin and till the fluid reaches outlet.
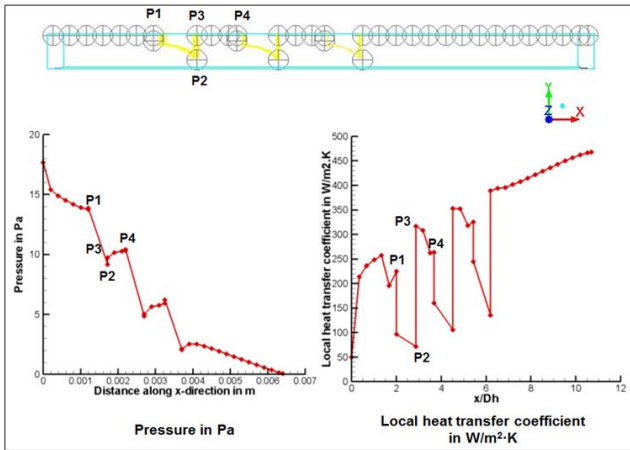
Fig .8. Pressure and local heat transfer coefficient for staggered ripsaw fin with thickness 0.0005 m

Table 2 shows the fluid flow and heat transfer values for the staggered arrangement of different fins. It has been found that the heat transfer and pressure drop increases for the staggered arrangement of the fins. It can be seen that the heat transfer rate is higher for ripsaw fin with thickness of 0.00005 m compared to the other cases. The obtained average Nusselt number is the highest for the inverted bolt fins and least for the ripsaw fins. The rectangular and triangular fins have similar values for the average Nusselt number and pressure drop. The Schimdt number is calculated based on the average temperature and it is found to be similar for all the cases studied. Due to the increase in pressure drop the friction factor is found to be the highest for inverted bolt fins followed by the rectangular fins. The ripsaw fin with thickness of 0.00005 m has the least friction factor.

Table 2. Fluid flow and heat transfer values for the staggered flow arrangement

Staggered arrangement				
Types	Rectangle fins	Triangle fins	Inverted bolt fins	Ripsaw fin with thickness 0.00005 m
Heat transfer rate (W)	0.481	0.478	0.482	0.494
Heat transfer surface area (m^2)	$2.256 \cdot 10^{-5}$	$2.205 \cdot 10^{-5}$	$2.233 \cdot 10^{-5}$	$2.262 \cdot 10^{-5}$
Heat transfer coefficient (W/m$^2 \cdot$K)	224.16	226.28	239.04	223.61
Average Nusselt number	3.205	3.235	3.418	3.197
Colburn j factor	0.016	0.016	0.017	0.016
Schimdt number	0.316	0.316	0.315	0.315
Friction factor f	0.894	0.725	0.996	0.522

There is a little increase in pressure drop compared to the uniform arrangement of the fins (Nagarajan et al. [11]). The ripsaw and the inverted bolt fins do not have noticeable increase in pressure drop. All the obtained pressure drop values are good for safe operation. Due to the smaller heat transfer surface area the effectiveness obtained is also less. There is increase in the effectiveness of the heat exchanger and the ripsaw fin with thickness of 0.00005 m is found to have the highest effectiveness. Table 3 shows the pressure drop and temperature values for the staggered arrangement.

Table 3. Pressure drop and temperature difference between the inlet and the outlet for the flow channels

	ΔP in reacting flow channel (Pa)	ΔT in reacting flow channel (K)	ΔT in helium flow channel (K)	Temperature gradient in reacting flow channel (K/mm)	Mass diffusivity in the reacting channel D_{AB} (m$^2 \cdot$s^{-1})	Effectiveness ε
Rectangular fins	28.41	135.13	55.58	20.90	$6.25 \cdot 10^{-6}$	0.544
Triangular fins	23.03	132.89	52.72	20.55	$6.26 \cdot 10^{-6}$	0.535
Inverted bolt fins	31.64	134.22	58.26	20.76	$6.27 \cdot 10^{-6}$	0.540
Ripsaw fin with thickness of 0.00005 m	16.59	137.35	59.85	21.24	$6.28 \cdot 10^{-6}$	0.553

V. CONCLUSION

The obtained average Nusselt number is higher for inverted bolt fins which is 3.418 followed by triangular fins which is 3.235. The obtained pressure drop for

the rectangular fins is higher compared to the triangular fins for similar heat transfer rate. For similar heat transfer rate the obtained pressure drop which is 16.59 Pa is less for the ripsaw fins compared to the other fins. Hence ripsaw fin with thickness of 0.00005 m is considered to be the best design with less pressure drop and reasonable heat transfer rate. The inverted bolt fins have the highest average Nusselt number followed by the triangular fins.

The values of the average Nusselt number for the triangular and the rectangular fins are very close. Even though the obtained average Nusselt number for the ripsaw fin with 0.00005 m thickness which is $(\overline{Nu})$ = 3.2 is less compared to the other fins, the obtained pressure drop for the ripsaw fins is the least of all the four fins which is 16.59 Pa. Hence the ripsaw fin thickness of 0.00005 m is selected as the best design with good heat transfer rate of 0.494 W and minimum pressure drop of 18.73 Pa.

REFERENCES

[1] Hesselgreaves, J. E. (2001). Compact Heat Exchangers Selection, Design and Operation. Oxford, UK: Elsevier Science Ltd.

[2] Kayansayan, N. (1994). Heat Transfer Characterization in Plate-Fin Tube Heat Exchangers. International Journal of Refrigeration, 17, pp. 49-57.

[3] Ranganayakulu, C. & Seetharamu. K.N. (1999). The Combined Effects of Wall Longitudinal Heat Conduction, Inlet Fluid Flow Non-Uniformity and Temperature Non-Uniformity in Compact Tube-Fin Heat Exchangers: A Finite Element Method. International Journal of Heat and Mass Transfer, 42, pp. 263-73.

[4] Wen, J. & Liu. (2004). Study of Flow Distribution and Its Improvement on the Header of Plate-Fin Heat Exchanger. Cryogenics, 44(11), pp. 823-831.

[5] Manglik, R. M. &. Bergles, A. E. (1995). Heat Transfer and Pressure Drop Correlations for the Rectangular Offset Strip Fin Compact Heat Exchanger. Experimental Thermal and Fluid Science, 10, pp. 171-80.

[6] Bhowmik, H., &. Lee, K. (2008). Analysis of Heat Transfer and Pressure Drop Characteristics in an Offset Strip Fin Heat Exchanger. International Communications in Heat and Mass Transfer, 36(3), pp. 259-263.

[7] Ma, T., Wang, Q. W., Zeng, M., Chen, Y., Liu, Y., & Nagarajan, V. (2012). Study on Heat Transfer and Pressure Drop Performances of Ribbed Channel in the High Temperature Heat Exchanger. Applied energy, 99, pp. 393-401.

[8] Schulte-Fischedick, J., Dreibigacker, V., & Tamme, R. (2007). An Innovative Ceramic High Temperature Plate-Fin Heat Exchanger for EFCC Processes. Applied Thermal Engineering, 27(8-9), pp. 1285-94.

[9] Monteiro, D. &. B., & Batista De Mello, P.E. (2012). Thermal Performance and Pressure Drop in a Ceramic Heat Exchanger Evaluated Using CFD Simulations. Energy, 45, pp. 489-496.

[10] Ponyavin, V., Chen, Y., Mohamed, T., Trabia, M.B., Hechanova, A.E., & Wilson, M. (2012). Design of a Compact Ceramic High-Temperature Heat Exchanger and Chemical Decomposer for Hydrogen Production. Heat Transfer Engineering, 33(10), pp. 853-70.

[11] Nagarajan, V., Chen, Y., Wang, Q., & Ma, T. (2014). Hydraulic and Thermal Performances of a Novel Configuration of High Temperature Ceramic Plate-Fin Heat Exchanger. Applied Energy, 113, pp. 589-602.

[12] SOLIDWORKS 2013., SOLIDWORKS Corp.

[13]   ANSYS Inc. (2011). ANSYS 14.5 user's guide.

[14] Patankar, S. (1980). Numerical Heat Transfer and Fluid Flow. New York.

[15] Manson, S. V. (1950). Correlations of Heat Transfer Data and Friction Data for Interrupted Plate Fins Staggered In Successive Rows.

Washington DC: National Advisory Committee for Aeronautics.

[16] Wieting, A. R. (1975). Empirical Correlations for Heat Transfer and Flow Friction Characteristics of Rectangular Offset-Fin-Plate-Fin Heat Exchanger. ASME, Int J. Heat Transfer, 97, pp. 480-490.